# Average Error Probability for UAV-RIS Enabled Short Packet Communications

Lai Wei, Kezhi Wang, *Member, IEEE,* Cunhua Pan, *Member, IEEE,* Maged Elkashlan, *Senior Member, IEEE*

*Abstract*—**This paper analyzes the performance of an aerial-empowered reconfigurable intelligent surface (RIS) aided communication system under finite channel blocklength. Firstly, we establish the system model of the UAV-RIS enabled short packet communication system and derive closed-form approximations for the cumulative distribution function (CDF) of the received signal-to-noise-ratio (SNR) of the ground user using a moment matching method. The approximation results match the simulation results very well under various conditions, providing simple method for and shedding light on performance evaluation for practical system. Secondly, we derive the average error probability of the UAV-RIS enabled short packet communication system in closed-form expressions, present the asymptotic analysis in the regime of high SNR and a large number of RIS elements and discuss the impact of transmit power and number of RIS elements on system performance, which provides insights into energy-efficient and cost-effective system design. Finally, we conduct Monte Carlo simulations to confirm the accuracy of our analytical and asymptotic results.**

*Index Terms*—**Unmanned aerial vehicle, reconfigurable intelligent surface, short packet communications**

## I. Introduction

Ultra-reliable low-latency communication (URLLC) is one of the main service categories in the future generations of wireless communications [1]. However, the stringent requirements of latency and reliability hinder the applications of URLLC. Recently, the reconfigurable intelligent surface (RIS) technology has attracted increasing research attentions in resolving the above challenges by improving the quality of received signals both cost-effectively and energy-efficiently. The recent research evaluated the effectiveness of deploying RIS to assist URLLC under different scenarios with finite channel blocklength. In [2] and [3], the authors analyzed the average decoding error probability and average data rate in

This work of Lai Wei was supported by China Scholarship Council. (*Corresponding author: Kezhi Wang and Cunhua Pan.*)

Lai Wei is with Department of Electronics, Peking University, Beijing 100871, China and School of Electronic Engineering and Computer Science, Queen Mary University of London, London E1 4NS, U.K. (e-mail: 598634680@qq.com).

Kezhi Wang is with Department of Computer Science, Brunel University London, Uxbridge, Middlesex, UB8 3PH (email: kezhi.wang@brunel.ac.uk). The work of Kezhi Wang was supported in part by the Horizon Europe COVER project (101086228).

Cunhua Pan is with the National Mobile Communications Research Laboratory, Southeast University, Nanjing 210096, China (email: cpan@seu.edu.cn). The work of Cunhua Pan was supported in part by the National Natural Science Foundation of China (Grant No. 62201137, 62331023).

Maged Elkashlan is with School of Electronic Engineering and Computer Science, Queen Mary University of London, London E1 4NS, U.K. (e-mail: maged.elkashlan@qmul.ac.uk).

RIS-aided URLLC systems. In [4], the authors investigated the average error probability of a RIS-aided URLLC system supported by wireless energy transfer technology. Moreover, the authors of [5] studied the throughput maximization in a RIS-aided multiple-input multiple-output (MIMO) wireless powered communication networks. Nevertheless, the existing works considered the case where the RIS is deployed at a fixed location, which restricts the application of the RIS-aided URLLC systems. This motivates us to consider the scenario where the RIS is deployed flexibly in the space to accommodate various requirements of URLLC systems.

In addition, it is well known that unmanned aerial vehicles (UAVs) can be a promising technology for future wireless networks. Additionally, it would be beneficial for equipping the UAVs with RIS to enhance the network coverage and user connectivity. Recently, there have been a few works considering the integration and coexistence of UAV and RIS. In [6], the authors analyzed the capacity of a RIS-assisted UAV network where the RIS is equipped on a high altitude airship. The work in [7] investigated the performance analysis and optimization of an integrated UAV-RIS relaying system. The authors of [8] studied a symbiotic UAV-RIS system, where the UAV was utilized to assist the RIS to reflect its signals as well as enhance the UAV transmission by using passive beamforming. In [9], the physical layer security of a UAV-RIS relaying system in the presence of multiple eavesdroppers is considered. In [10], the authors investigated the optimization problem of passive beamforming, transmission blocklength and UAV positioning of a RIS-aided wireless system with a mobile UAV relay. In [11], the optimization of beamforming and phase shift design is considered in a UAV-RIS-enabled wireless system. However, to the best of the authors' knowledge, the performance analysis of UAV-RIS assisted URLLC systems under finite channel blocklength has not been investigated yet.

Against the above background, we study the performance of the UAV-RIS enabled URLLC system with short packet communications. Compared with the existing works, we have jointly considered the impacts of short-packet communications, randomness of UAV and the effect of RIS. Moreover, we have conducted asymptotic analysis and provided some insights. Specifically, we analyze the average error probability under finite channel blocklength. By using a moment matching method to approximate the received SNR as a Gamma random variable, we first derive closed-form approximations for the cumulative distribution function (CDF) of the received SNR of the ground user. Then, we obtain the average error probability of the UAV-RIS enabled URLLC system in closed-form expressions. Next, we present the asymptotic analysis when the

normalized transmit power and the number of RIS elements are sufficiently large, the trade-off between increasing BS's transmit power and equipping UAV with more RIS elements is discussed. Finally, Monte Carlo simulations are carried out to evaluate the accuracy of the analytical and asymptotic results.

*Notations*: We use $f(x)$ and $F(x)$ to denote the probability density function (PDF) and cumulative distribution function (CDF), respectively. $Q(x) = \int_x^\infty e^{-\frac{t^2}{2}} \mathrm{d}t$ denotes the Q-function. $\gamma(a,z) = \int_0^z z^{a-1} e^{-z} \mathrm{d}z$ is the lower incomplete gamma function and $\Gamma(\cdot)$ is the Gamma function. $_pF_q(\mathbf{a}_p; \mathbf{b}_q; z)$ is the generalized hypergeometric function [12, eq. (9.14.1)]. $\mathbb{E}$ represents the mathematical expectation operator.

## II. SYSTEM MODEL

As shown in Fig. 1, we consider a scenario where a single-antenna ground user communicates with a single-antenna base station (BS) under finite channel blocklength through a RIS mounted on a UAV. The UAV acts as a passive relay and carries a rectangular RIS which consists of $N$. For the sake of simplicity, we consider that the distance between the BS and the ground user $D$ is sufficiently large, thus the direct link between the BS and the ground user is negligibly weak. Furthermore, we assume that the UAV-RIS flies randomly inside a spherical shell with inner radius $R_1$ and outer radius $R_2$ while the BS is located at the center of the sphere. To avoid collision onto the obstacles and in case of losing the control signal from the BS, it is assumed that the UAV will not fly into the inner sphere or fly out of the outer sphere. Throughout this paper, we use $d_R$ to denote the distance between the BS and the UAV-RIS, whereas $d_U$ to denote the distance between the UAV-RIS and the ground user. In addition, we assume that the BS-UAV and the UAV-user links suffer from Rician fading with $h_i$ and $g_i$ denoting the small scale fading of the BS-UAV and the UAV-user channel and $i$ denoting the index of RIS element, respectively.



Fig. 1.  System model of the UAV-RIS enabled wireless system with short packet communications. The RIS consists of $N$ elements and is mounted on a UAV which flies randomly inside a shell with inner radius $R_1$ and outer radius $R_2$. The length of the direct link between the BS and the user is $D$.

## III. AVERAGE ERROR PROBABILITY ANALYSIS

In the following analysis, we assume that the BS aims to successfully transmit $B$ information bits over $M$ channel uses. Therefore, the coding rate of the short packet communications is given by $R = B/M$.

### A. Received SNR Analysis and Approximation

With optimal phase shift of the $i$-th $(i = 1, 2, \cdots, N)$ RIS element, the received SNR at the ground user is given by

$$\gamma_U = \rho(d_R d_U)^{-\alpha} \left( \sum_{i=1}^N |g_i| \, |h_i| \right)^2, \tag{1}$$

where $\rho = \frac{P_{BS}}{\sigma^2}$ is the normalized transmit power of the BS and $\alpha$ denotes the pathloss factor.

For the sake of simplicity, we rewrite the channel coefficients in more compact forms as follows

$$\mathbf{h} \triangleq [h_1, \cdots, h_N]^T = \sqrt{\frac{\beta_1}{\beta_1 + 1}} \bar{\mathbf{h}} + \sqrt{\frac{1}{\beta_1 + 1}} \widetilde{\mathbf{h}},$$
$$\mathbf{g} \triangleq [g_1, \cdots, g_N]^T = \sqrt{\frac{\beta_2}{\beta_2 + 1}} \bar{\mathbf{g}} + \sqrt{\frac{1}{\beta_2 + 1}} \widetilde{\mathbf{g}}, \tag{2}$$

where $\beta_1$ and $\beta_2$ denote the Rician factors, $\bar{\mathbf{h}}$ and $\widetilde{\mathbf{h}}$ denote the Line-of-Sight (LoS) and None-Line-of-Sight (NLOS) components of $\mathbf{h}$ while $\bar{\mathbf{g}}$ and $\widetilde{\mathbf{g}}$ denote the LoS and NLoS components of $\mathbf{g}$, respectively [9].

From the above analysis, we directly infer that $|h_i|$ is a Rician random variable with noncentrality parameter $\nu_1 = \frac{\beta_1}{\beta_1+1}$ and scale parameter $\sigma_1 = \sqrt{\frac{1}{2(\beta_2+1)}}$ namely, $|h_i| \sim$ Rician$(\nu_1, \sigma_1)$ . Similarly, we have $|g_i| \sim$ Rician$(\nu_2, \sigma_2)$ with $\nu_2 = \frac{\beta_2}{\beta_2+1}$ and $\sigma_2 = \sqrt{\frac{1}{2(\beta_2+1)}}$.

Defining $\xi_i = |g_i| \, |h_i|$, we further rewrite $\gamma_U$ as

$$\gamma_U = \rho(d_R d_U)^{-\alpha} \left( \sum_{i=1}^N \xi_i \right)^2 \triangleq \rho(d_R d_U)^{-\alpha} Z. \tag{3}$$

Leveraging a moment matching method [2], the random variable $Z \triangleq (\sum_{i=1}^N \xi_i)^2$ can be approximated by a Gamma distributed random variable with shape parameter $\hat{k} = \frac{\mathbb{E}[Z]^2}{\mathbb{E}[Z^2] - \mathbb{E}[Z]^2}$ and scale parameter $\hat{\theta} = \frac{\mathbb{E}[Z^2] - \mathbb{E}[Z]^2}{\mathbb{E}[Z]}$. With the help of the moments of random variable $\xi_i$, the first and second order moments of random variable $Z$ can be calculated as follows

$$\mathbb{E}[Z] = \sum_{i=1}^N \mathbb{E}\left[ \xi_i^2 \right] + \sum_{\substack{i,j=1 \\ i \neq j}}^N \mathbb{E}[\xi_i] \, \mathbb{E}[\xi_j],$$

$$\mathbb{E}[Z^2] = \mathbb{E}\left[ \left( \sum_{i=1}^N \xi_i^2 + \sum_{\substack{i,j=1 \\ i \neq j}}^N \xi_i \xi_j \right)^2 \right]. \tag{4}$$

Moreover, the $m$-th order moment of $\xi_i$ can be calculated leveraging the $m$-th order moments of $|g_i|$ and $|h_i|$ which can be expressed as

$$\mathbb{E}[|h_i|^m] = \sigma_1^m 2^{m/2} \Gamma(1 + m/2) L_{m/2}(-\nu_1^2 / 2\sigma_1^2),$$
$$\mathbb{E}[|g_i|^m] = \sigma_2^m 2^{m/2} \Gamma(1 + m/2) L_{m/2}(-\nu_2^2 / 2\sigma_2^2), \tag{5}$$

where $L_q(z) = {}_1F_1(-q; 1; z)$ denotes the Laguerre polynomial with the $q$-th order.

After some tedious mathematical derivations, we can obtain the approximated shape parameter $\hat{k}$ and scale parameter $\hat{\theta}$. Therefore, the CDF of $\gamma_U$ conditioned on $d_R$ and $d_U$ can be approximated as follows

$$F_{\gamma_U}(x|d_R, d_U) \approx \frac{1}{\Gamma(\hat{k})}\gamma(\hat{k}, \frac{x}{\rho(d_R d_U)^{-\alpha}\hat{\theta}}). \quad (6)$$

In sphere coordinates, the position of the UAV can be expressed as $(r, \theta, \varphi)$ where $r = d_R$ is the distance between the UAV and the BS, and $\theta \in [0, 2\pi]$ and $\varphi \in [0, \pi/2]$ denote the azimuth and elevation angles, respectively. Similarly, we denote the position of the ground user as $(D, \theta_U, \varphi_U)$. With the aforementioned preliminaries, we obtain the expression of $d_U$ as

$$d_U = \sqrt{r^2 + D^2 - 2rD[\sin\varphi\sin\varphi_U\cos(\theta - \theta_U) + \cos\varphi\cos\varphi_U]}. \quad (7)$$

Since we have $r = d_R$ and $d_U$ is also a function of $r, \theta, \varphi$ in sphere coordinate, the unconditional CDF of the ground user's received SNR can be given by

$$F_{\gamma_U}(x) = \mathbb{E}[F_{\gamma_U}(x|r, \theta, \varphi)], \quad (8)$$

where the mathematical expectation is taken over random variables $r$, $\theta$, and $\varphi$.

To the best of the authors' knowledge, it is quite challenging to derive the exact expression of $F_{\gamma_U}(x)$. The difficulty stems from the randomness of $d_U$. To tackle this issue, we first use Gauss-Chebyshev quadrature approximation method [20] to calculate $F_{\gamma_U}(x)$. Specifically, the mathematical expression of unconditional CDF of the ground user's received SNR in (8) could be further rewritten as

$$F_{\gamma_U}(x) = \int_0^{\frac{\pi}{2}}\int_0^{2\pi}\int_{R_1}^{R_2} F_{\gamma_U}(x|r, \theta, \varphi)f(r, \theta, \varphi)\mathrm{d}r\mathrm{d}\theta\mathrm{d}\varphi$$
$$= \int_0^{\frac{\pi}{2}}\int_0^{2\pi}\int_{R_1}^{R_2} F_{\gamma_U}(x|r, \theta, \varphi)\frac{3r^2}{R_2^3 - R_1^3} \cdot \frac{1}{2\pi} \cdot \frac{2}{\pi}\mathrm{d}r\mathrm{d}\theta\mathrm{d}\varphi. \quad (9)$$

Leveraging change of variables, we obtain

$$F_{\gamma_U}(x) = \int_{-1}^1\int_{-1}^1\int_{-1}^1 g_{\gamma_U}(x|u, v, s)\mathrm{d}u\mathrm{d}v\mathrm{d}s, \quad (10)$$

where

$$g_{\gamma_U}(x|u, v, s) \triangleq \frac{3(R_2 - R_1)}{8(R_2^3 - R_1^3)}$$
$$\times F_{\gamma_U}\left(x \Big| \frac{R_2 - R_1}{2}u + \frac{R_2 + R_1}{2}, \pi v + \pi, \frac{\pi}{4}s + \frac{\pi}{4}\right) \quad (11)$$
$$\times \left(\frac{R_2 - R_1}{2}u + \frac{R_2 + R_1}{2}\right)^2.$$

Finally, using Gauss-Chebyshev quadrature approximation method, the unconditional CDF of the ground user's received SNR could be expressed as follows

$$F_{\gamma_U}(x) \approx \left(\frac{\pi}{W}\right)^3 \times$$
$$\sum_{i,j,k=1}^W \sqrt{(1 - u_i^2)(1 - v_j^2)(1 - s_k^2)} \cdot g_{\gamma_U}(x|u_i, v_j, s_k), \quad (12)$$

where $W$ is the number of samples, $u_i \triangleq \cos\left(\frac{2i-1}{2W}\pi\right)$, $v_j \triangleq \cos\left(\frac{2j-1}{2W}\pi\right)$ and $s_k \triangleq \cos\left(\frac{2k-1}{2W}\pi\right)$.

As will be discussed in Section IV, the unconditional CDF obtained from Gauss-Chebyshev approximation method matches the exact CDF very well when system parameters take various values.

However, although the Gauss-Cehbyshev approximation provides an efficient method for numerical evaluation of the system performance, it is still quite challenging to find the impact of system parameters such as transmit power and number of RIS elements on system performance. To further discuss such issue, we consider a scenario where the mathematical expression of unconditional CDF could be further simplified. Specifically, we assume that the distance between the BS and the ground user is much larger than that between the BS and the UAV-RIS such that $R_2 \ll D$ holds. In such context, we have $d_U \approx D$ [13]. Note that this assumption also gives a lower bound of the performance of the system. With the help of [14, eq. (1)], the CDF of the SNR can be approximated as

$$F_{\gamma_U}(x) = \mathbb{E}[F_{\gamma_U}(x|r, \theta, \varphi)] \approx \int_{R_1}^{R_2} F_{\gamma_U}(x|r)f(r)\mathrm{d}r$$
$$= \int_{R_1}^{R_2} \frac{3r^2}{R_2^3 - R_1^3} \cdot \frac{1}{\Gamma(\hat{k})}\gamma(\hat{k}, \Omega x r^\alpha)\mathrm{d}r, \quad (13)$$

where $\Omega \triangleq \frac{1}{\rho D^{-\alpha}\hat{\theta}}$.

Finally, utilizing [12, eq. (8.351.2), (9.210.1)], [15, eq. (1.14.1.8)] and variable transformations, we obtain the approximation of $F_{\gamma_U}(x)$ in closed form as follows

$$F_{\gamma_U}(x) \approx \frac{3}{(R_2^3 - R_1^3)\Gamma(\hat{k})}\int_{R_1^\alpha}^{R_2^\alpha}\frac{1}{\alpha}t^{\frac{3}{\alpha}-1}\gamma(\hat{k}, \frac{xt}{\rho D^{-\alpha}\hat{\theta}})\mathrm{d}t$$
$$= \eta x^{\hat{k}}\int_{R_1^\alpha}^{R_2^\alpha}t^{\hat{k}+\frac{3}{\alpha}-1}e^{-\Omega xt}{}_1F_1(1; \hat{k}+1; \Omega xt)\mathrm{d}t$$
$$= \eta x^{\hat{k}}\left(R_2^{\alpha\hat{k}+3}\mathcal{F}(x, R_2^\alpha) - R_1^{\alpha\hat{k}+3}\mathcal{F}(x, R_1^\alpha)\right), \quad (14)$$

where $\eta \triangleq \frac{3\Omega^{\hat{k}}}{\alpha\hat{k}(\hat{k}+\frac{3}{\alpha})(R_2^3-R_1^3)\Gamma(\hat{k})}$ and the function $\mathcal{F}(x, t)$ is defined as

$$\mathcal{F}(x, t) = {}_2F_2(\hat{k}+\frac{3}{\alpha}, \hat{k}; \hat{k}+\frac{3}{\alpha}+1, \hat{k}+1; -\Omega xt). \quad (15)$$

### B. Average Error Probability Analysis

In finite blocklength coding regime, the average decoding error probability given a transmission rate $R$ can be calculated as [16]

$$\bar{\epsilon} = \mathbb{E}\left[Q\left(\frac{C(\gamma) - R}{\sqrt{V(\gamma)/M}}\right)\right], \quad (16)$$

where the expectation is taken over the received SNR $\gamma$. Moreover, $C(\gamma) = \log_2(1 + \gamma)$ is channel capacity and $V(\gamma) = \left(1 - \frac{1}{(1+\gamma)^2}\right)(\log_2(e))^2$ denotes channel dispersion.

Due to the complicated structure of Q-function, it is intractable to obtain a closed-form expression for the average

decoding error probability. Therefore, we leverage a linear approximation of Q-function as follows [17]

$$
\begin{aligned}
Q\left(\frac{C(\gamma) - R}{\sqrt{V(\gamma)/M}}\right) &\approx \Xi(\gamma) \\
&= \begin{cases} 1, & \gamma \leq \zeta \\ \frac{1}{2} - \nu\sqrt{M}(\gamma - \theta), & \zeta < \gamma < \xi, \\ 0, & \gamma \geq \xi \end{cases}
\end{aligned} \tag{17}
$$

where $\nu = \frac{1}{\sqrt{2\pi(2^{2R}-1)}}$, $\theta = 2^R - 1$, $\zeta = \theta - \frac{1}{2\nu\sqrt{M}}$ and $\xi = \theta + \frac{1}{2\nu\sqrt{M}}$, respectively.

Using the above linear approximation of Q-function and integral by part, the average decoding error probability can be approximated as [18]

$$
\bar{\epsilon} \approx \int_0^{+\infty} \Xi(x) f_{\gamma_U}(x)\mathrm{d}x = \nu\sqrt{M}\int_\zeta^\xi F_{\gamma_U}(x)\mathrm{d}x. \tag{18}
$$

Finally, by substituting (14) into (18) and leveraging [15, eq. (1.16.1.1)], we obtain the average decoding error probability in closed form as follows

$$
\bar{\epsilon} \approx \frac{\eta\nu\sqrt{M}}{\hat{k}+1}\left(R_2^{\alpha\hat{k}+3}\mathcal{G}(\xi,\zeta,R_2^\alpha) - R_1^{\alpha\hat{k}+3}\mathcal{G}(\xi,\zeta,R_1^\alpha)\right), \tag{19}
$$

where

$$
\mathcal{G}(x,y,t) \triangleq x^{\hat{k}+1}\mathcal{H}(x,t) - y^{\hat{k}+1}\mathcal{H}(y,t), \tag{20}
$$

and

$$
\mathcal{H}(x,t) \triangleq {}_3F_3(\hat{k}+\frac{3}{\alpha}, \hat{k}, \hat{k}+1; \hat{k}+\frac{3}{\alpha}+1, \hat{k}+1, \hat{k}+2; -\Omega xt). \tag{21}
$$

### C. Asymptotic Analysis

**Theorem 1.** *At high SNR regime where $\rho$ is sufficiently large, the average decoding error probability can be given by*

$$
\bar{\epsilon}_\rho^\infty \approx \frac{\eta\nu\sqrt{M}}{\alpha(\hat{k}+1)}(R_2^{\alpha\hat{k}+3} - R_1^{\alpha\hat{k}+3})(\xi^{\hat{k}+1} - \zeta^{\hat{k}+1}). \tag{22}
$$

*Proof.* According to [12, eq. (8.354.1)], at high SNR regime, the conditional received SNR can be approximated as

$$
\begin{aligned}
F_{\gamma_U}^{\rho\to\infty}(x|r) &\approx \frac{1}{\Gamma(\hat{k})}\gamma(\hat{k}, \frac{xr^\alpha}{\rho D^{-\alpha}\hat{\theta}}) \\
&= \frac{1}{\Gamma(\hat{k})}\sum_{n=0}^{+\infty}\frac{(-1)^n(\Omega xr^\alpha)^{\hat{k}+n}}{n!(\hat{k}+n)} \approx \frac{(\Omega xr^\alpha)^{\hat{k}}}{\hat{k}\Gamma(\hat{k})}.
\end{aligned} \tag{23}
$$

Therefore, the unconditional SNR can be approximated as

$$
\begin{aligned}
F_{\gamma_U}^{\rho\to\infty}(x) &\approx \int_{R_1}^{R_2}\frac{(\Omega xr^\alpha)^{\hat{k}}}{\hat{k}\Gamma(\hat{k})}f(r)\mathrm{d}r \\
&= \frac{3\Omega^{\hat{k}}(R_2^{\alpha\hat{k}+3} - R_1^{\alpha\hat{k}+3})}{\alpha\hat{k}(\alpha\hat{k}+3)(R_2^3 - R_1^3)\Gamma(\hat{k})}x^{\hat{k}}.
\end{aligned} \tag{24}
$$

Finally, by substituting (24) into (18), we obtain (22). $\square$

**Remark 1.** *A careful investigation on the above equation reveals that $\bar{\epsilon} \to 0$ when $\rho \to +\infty$, which can be directly obtained by substituting $\lim_{\rho\to\infty}\Omega = \lim_{\rho\to\infty}\eta = 0$ into*

*equation (22). This result shows that the average decoding error probability can be limited to arbitrarily small by increasing the transmit power of the BS.*

**Theorem 2.** *As the number of RIS elements is sufficiently large, equation (19) also characterizes the asymptotic average error probability, namely,*

$$
\bar{\epsilon}_N^\infty \approx \frac{\eta\nu\sqrt{M}}{\alpha(\hat{k}+1)}(R_2^{\alpha\hat{k}+3} - R_1^{\alpha\hat{k}+3})(\xi^{\hat{k}+1} - \zeta^{\hat{k}+1}). \tag{25}
$$

*Proof.* From (4) we observe that the shape parameter $\hat{k}$ and the scale parameter $\hat{\theta}$ increase monotonically with respect to $N$. Hence, we have $\lim_{N\to\infty}\hat{k} = \infty$ and $\lim_{N\to\infty}\hat{\theta} = \infty$. Furthermore, according to [19], for sufficiently large $\hat{k}$, we have the following asymptotic expansion of $\gamma(\hat{k}, \Omega xr^\alpha)$

$$
\lim_{\hat{k}\to\infty}\gamma(\hat{k}, \Omega xr^\alpha) \sim (\Omega xr^\alpha)^{\hat{k}}e^{-\Omega xr^\alpha}\sum_{n=0}^{+\infty}\frac{(\Omega xr^\alpha)^n}{(\hat{k})_{n+1}}, \tag{26}
$$

where $(\cdot)_n$ is the Pochhammer symbol. As $\hat{k}$ is sufficiently large, the items with $n > 0$ in the above summations are negligible due to $\lim_{\hat{k}\to\infty}\frac{\Omega xr^\alpha}{\hat{k}} = 0$. In addition, it is obvious that $\hat{\theta} \to \infty$ leads to $\Omega \to 0$. Therefore, we obtain

$$
\lim_{N\to\infty}\gamma(\hat{k}, \Omega xr^\alpha) \sim \frac{1}{\hat{k}}(\Omega xr^\alpha)^{\hat{k}}e^{-\Omega xr^\alpha} \approx \frac{1}{\hat{k}}(\Omega xr^\alpha)^{\hat{k}}. \tag{27}
$$

The proof is then complete after some similar mathematical manipulations as in **Theorem 1**. $\square$

**Remark 2.** *Equation (25) characterizes the asymptotic impact of the number of RIS elements on the average error probability. By substituting $\lim_{N\to\infty}\hat{k} = \infty$ into (25) one can observe from (25) that $\bar{\epsilon} \to 0$ when $N \to \infty$, namely, the average error probability vanishes when the number of RIS elements $N$ is sufficiently large.*

Based on **Remark 2** and recalling the conclusion in **Remark 1**, the performance of the system could be enhanced by either increasing the power consumption of BS or equipping more RIS elements on the UAV. One may directly figure out that increasing the number of RIS elements is a more promising method in URLLC compared with increasing the transmit power of the BS, because the former method does not lead to more power consumption of BS. However, carrying more RIS elements causes more power consumption of the UAV. Therefore, if the additional power consumption of the UAV is no more than that of the BS, increasing the number of RIS elements will be more cost-effective and energy-efficient than increasing BS's transmit power. We summarize this conclusion in the following **Remark 3**.

**Remark 3.** *Given the number of RIS elements $N$, we denote average decoding error probability $\bar{\epsilon} = \mathcal{E}(\rho|N)$ as a function of BS's transmit power $\rho$, and $\rho = \mathcal{E}^{-1}(\bar{\epsilon}|N)$ is its inverse function. As the number of RIS elements increases by one, the performance gain of the system indicated by the corresponding decrease of error probability could be given as $\Delta\bar{\epsilon} = \mathcal{E}(\rho|N) - \mathcal{E}(\rho|N+1)$. Assuming the number of RIS elements remains unchanged, to achieve a same performance gain, the BS's power budget should increase by $\delta\rho = \mathcal{E}^{-1}(\bar{\epsilon}+\Delta\bar{\epsilon}) - \rho$.*

*Suppose carrying one more RIS element results in an increase of energy consumption $\delta E$ of the UAV, increasing one more RIS elements is energy-efficient and cost-effective if and only if $\delta \rho > \delta E$ holds.*
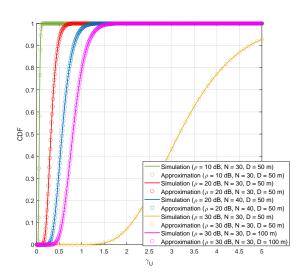
## IV. SIMULATION RESULTS

Unless otherwise specified, the parameters are set as follows: $B = 500$ bits, $M = 500$ channel uses, $R_1 = 8$ m, $R_2 = 10$ m, $D = 150$ m, $\alpha = 2$, $f = 2.4$ GHz, $\delta_c = \delta_r = \lambda/4$ and $\beta_1 = \beta_2 = 3$ dB. All the Monte Carlo simulations are conducted by averaging over $10^7$ channel realizations.

Fig. 2 illustrates the empirical CDF of the ground user's received SNR and its approximation based on Gauss-Chebyshev quadrature. It is shown that the Gauss-Chebyshev quadrature approximation results match the exact CDF in various parameters settings. Therefore, Gauss-Chebyshev approximation is an efficient method for numerical evaluation of system performance.

In Fig. 3, we present the approximate and empirical CDFs of the received signal under different normalized transmit power $\rho$ and the number of RIS elements $N$. Fig. 3 shows that the proposed moment matching method provides a precise approximation to the distribution of the received SNR, which is sufficiently general to accommodate various circumstances.

Fig. 4 depicts the average error probability versus the blocklength $M$ with the information package size being $B = 500$ bits. It can be readily found that an increase in the blocklength makes a decrease in the average error probability since a larger blocklength leads to a lower transmission rate, which guarantees the communications to be more reliable. The fact that lower transmission rate leading to lower error probability indicates the trade-off between reliability and efficiency in the UAV-RIS aided short packet communications, which should be carefully tackled in URLLC scenarios. Moreover, one can notice that the more RIS elements are equipped, the lower error probability are obtained, which demonstrates that the deployment of RIS can enhance the performance of short packet communications systems.

In Fig. 5 and Fig. 6, we examine the average error probability versus the normalized transmit power and the number of RIS elements, respectively. Note that in both figures, the circles marked as *Analysis* depict the results from directly calculating the numerical integration (16), while the diamonds labeled as *Approximation* represent the results derived by (19). Due to computational complexity, the simulation, analysis and approximation results are constrained to be no smaller than the order of $10^{-6}$, which generally accommodates most of the reliability requirements for URLLC applications. From Fig. 5 and Fig. 6, we observe that the analysis and approximation results are consistent with the simulation results. Moreover, the asymptotic results show that the average error probability vanishes quickly as the transmit power or the number of RIS elements increases. Therefore, as far as the condition in **Remark 3** is met, deploying RIS will be more cost-effective and energy-efficient compared with increasing the BS's power budget.



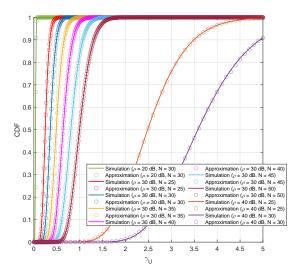Fig. 2. Gauss-Chebyshev Quadrature Approximate and empirical CDF of received SNR in various parameters settings.



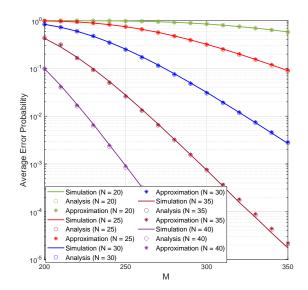Fig. 3. Approximate and empirical CDF of received SNR.



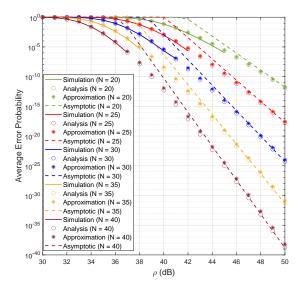Fig. 4. Average error probability versus blocklength $M$.

Fig. 5. Average error probability versus the normalized transmit power $\rho$.
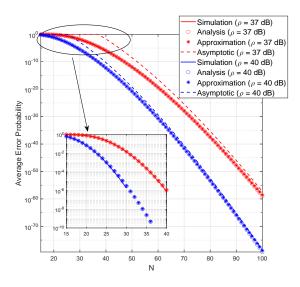


Fig. 6. Average error probability versus the number of RIS elements $N$.

## V. CONCLUSION

This paper analyzes the average error probability of a UAV-RIS enabled wireless system with short packet communications. We derive closed-form approximations for the average error probability under finite channel blocklength. The proposed approximation method provides a simple tool for and shedding light on performance evaluation for practical system. Analytical and simulation results reveal that the integration of UAV and RIS is a potential solution to enhance the performance of URLLC systems. Moreover, the asymptotic analysis unveils that the average error probability vanishes as either the transmit power or the number of RIS elements is sufficiently large. It is also shown that if the additional power consumption of equipping one more RIS elements on the UAV is small enough, the deployment of RIS will be more cost-effective and energy-efficient. Therefore, RIS will be a promising technique for supporting short packet communications in wireless networks.

## REFERENCES

[1] X. Sun, S. Yan, N. Yang, Z. Ding, C. Shen and Z. Zhong, "Short-packet downlink transmission with non-orthogonal multiple access," *IEEE Trans. Wireless Commun.*, vol. 17, no. 7, pp. 4550-4564, July 2018.
[2] H. Ren, K. Wang and C. Pan, "Intelligent reflecting surface-aided URLLC in a factory automation scenario," *IEEE Trans. Commun.*, vol. 70, no. 1, pp. 707-723, Jan. 2022.
[3] R. Hashemi, S. Ali, N. H. Mahmood and M. Latva-aho, "Average rate and error probability analysis in short packet communications over RIS-aided URLLC systems," *IEEE Trans. Veh. Technol.*, vol. 70, no. 10, pp. 10320-10334, Oct. 2021.
[4] B. Zhang, K. Wang, K. Yang and G. Zhang, "IRS-assisted short packet wireless energy transfer and communications," *IEEE Wireless Commun. Lett.*, vol. 11, no. 2, pp. 303-307, Feb. 2022.
[5] S. Gong, C. Xing, S. Wang, L. Zhao and J. An, "Throughput maximization for intelligent reflecting surface aided MIMO WPCNs with different DL/UL reflection patterns," *IEEE Trans. Signal Process.*, vol. 69, pp. 2706-2724, 2021.
[6] M. Al-Jarrah, E. Alsusa, A. Al-Dweik and D. K. C. So, "Capacity analysis of IRS-based UAV communications with imperfect phase compensation," *IEEE Wireless Commun. Lett.*, vol. 10, no. 7, pp. 1479-1483, July 2021.
[7] T. Shafique, H. Tabassum and E. Hossain, "Optimization of wireless relaying with flexible UAV-borne reflecting surfaces," *IEEE Trans. Commun.*, vol. 69, no. 1, pp. 309-325, Jan. 2021.
[8] M. Hua, L. Yang, Q. Wu, C. Pan, C. Li and A. L. Swindlehurst, "UAV-assisted intelligent reflecting surface symbiotic radio system," *IEEE Trans. Wireless Commun.*, vol. 20, no. 9, pp. 5769-5785, Sept. 2021.
[9] W. Wang, H. Tian and W. Ni, "Secrecy performance analysis of IRS-aided UAV relay system," *IEEE Wireless Commun. Lett.*, vol. 10, no. 12, pp. 2693-2697, Dec. 2021.
[10] A. Ranjha and G. Kaddoum, "URLLC facilitated by mobile UAV relay and RIS: a joint design of passive beamforming, blocklength, and UAV positioning," *IEEE Internet Things J.*, vol. 8, no. 6, pp. 4618-4627, Mar. 15, 2021.
[11] Y. Li, C. Yin, T. Do-Duy, A. Masaracchia and T. Q. Duong, "Aerial reconfigurable intelligent surface-enabled URLLC UAV systems," *IEEE Access*, vol. 9, pp. 140248-140257, 2021.
[12] I. S. Gradshteyn and I. M. Ryzhik, *Table of integrals, series, and products*. Waltham, MA, USA: Academic, 2014.
[13] J. Ye, A. Kammoun and M. -S. Alouini, "Spatially-distributed RISs vs relay-assisted systems: a fair comparison," *IEEE Open J. Commun. Soc.*, vol. 2, pp. 799-817, 2021.
[14] K. Wang, H. Lei, G. Pan, C. Pan and Y. Cao, "Detection performance to spatially random UAV using the ground vehicle," *IEEE Trans. Veh. Technol.*, vol. 69, no. 12, pp. 16320-16324, Dec. 2020.
[15] A. P. Prudnikov, J. A. Bryčkov, and O. I. Maričev, *Integrals and series. vol. 3, more special functions*, New York, NY, USA: Gordon Breach, 2003.
[16] Y. Polyanskiy, H. V. Poor and S. Verdu, "Channel coding rate in the finite blocklength regime," *IEEE Trans. Inf. Theory*, vol. 56, no. 5, pp. 2307-2359, May 2010.
[17] B. Makki, T. Svensson and M. Zorzi, "Finite block-length analysis of the incremental redundancy HARQ," *IEEE Wireless Commun. Lett.*, vol. 3, no. 5, pp. 529-532, Oct. 2014.
[18] Y. Gu, H. Chen, Y. Li and B. Vucetic, "Ultra-reliable short-packet communications: half-duplex or full-duplex relaying?," *IEEE Wireless Commun. Lett.*, vol. 7, no. 3, pp. 348-351, June 2018.
[19] N. M. TEMME, "Uniform asymptotic expansions of the incomplete gamma functions and the incomplete beta functions", *Ibid.*, 29 (1975), pp. 1109-1114.
[20] Do. D and Le. C, "Ergodic capacity computation in cognitive radio aided non-orthogonal multiple access systems," *Bulletin of Electrical Engineering and Informatics*, v. 11, n. 1, p. 270-277, Feb. 2022.